Letter

Dynamical emergence of a Kosterlitz-Thouless transition in a disordered Bose gas following a quench

Thibault Scoquart[1,2] Dominique Delande[1] and Nicolas Cherroret[1]

[1]*Laboratoire Kastler Brossel, Sorbonne Université, CNRS, ENS-PSL University, Collège de France; 4 Place Jussieu, 75005 Paris, France*

[2]*Institut für Theorie der Kondensierten Materie, Karlsruhe Institute of Technology, 76128 Karlsruhe, Germany*

(Received 16 May 2022; accepted 25 July 2022; published 11 August 2022)

We study the dynamical evolution of a two-dimensional Bose gas after a disorder potential quench. Depending on the initial conditions, the system evolves either to a thermal or a superfluid state. Using extensive quasiexact numerical simulations, we show that the two phases are separated by a Kosterliz-Thouless transition. The thermalization time is shown to be longer in the superfluid phase, but no critical slowing down is observed at the transition. The long-time phase diagram is well reproduced by a simple theoretical model. The spontaneous emergence of Kosterlitz-Thouless transitions following a quench is a generic phenomenon that should arise both in the context of nonequilibrium quantum gases and in the context of nonlinear classical wave systems.

DOI: 10.1103/PhysRevA.106.L021301

Following a quench, ergodic quantum systems experience a progressive loss of memory of their initial state. At a long time a thermal equilibrium establishes, governed by a few conserved quantities [1,2]. This ubiquitous phenomenon arises, in particular, in isolated systems, which act as a thermal bath for their subparts as formalized by the eigenstate thermalization hypothesis [3–5]. Despite the rather generic character of thermalization, it has been shown that its transient dynamics could be very rich. For certain far-from-equilibrium initial states, e.g., the postquench correlations functions of a quantum gas can display a universal spatiotemporal scaling [6–8]. Near-integrable systems also exhibit a slow prethermal dynamics [9–12], characterized by a generalized Gibbs ensemble [13,14]. Theoretically, descriptions of the full evolution of a quantum system from its early- to late-time dynamics have been proposed in a few cases [15–18], but this problem remains, in general, largely unexplored.

An important ingredient that may significantly impact the quench dynamics of an isolated system is spatial disorder. The role of disorder has been, for instance, addressed in the context of strongly interacting systems where the phenomenon of many-body localization prevents the emergence of a thermal state [19]. Initially described in one-dimensional geometries [20,21], many-body localization has also been recently touched upon in two dimensions (2D) [22–25]. In parallel, the ergodic regime has been explored in weakly interacting disordered Bose gases where it was shown that at transient times the competition between disorder and interactions can destroy localization effects [26–29] or drive the gas to a prethermal state [30,31].

Another central question in nonequilibrium physics is the possibility for coherent condensatelike structures to spontaneously emerge in an isolated system after a quench, a phenomenon that depends on dimensionality and occurs for specific initial conditions [32–39]. In practice, the dynamical formation of condensates has been much studied in the context of nonlinear optics where an optical field, analogous to a degenerate Bose gas, obeys a time-dependent nonlinear Schrödinger equation. Such dynamical condensation has been explored in atomic vapors [40,41] and in multimode fibers [42–44]. In these works, the effective spatial dimension was 2, and signatures of condensation were observed either due to the presence of a spatial confinement [42–44] or because the dynamics was probed at a finite time [40,41]. In 2D infinite space, however, no *true* condensation is expected at a long time, but rather a Kosterlitz-Thouless (KT) transition [45]. For homogeneous quantum gases at equilibrium, the KT transition has been observed in liquid helium [46] and with cold atoms [47–51]. In contrast, its spontaneous emergence in isolated systems following a quench is still elusive, although progress has been recently made in that direction [52,53]. Studies of the KT transition in the presence of disorder, on the other hand, remain scarce [54–57].

In this Letter, we demonstrate the spontaneous emergence of a KT transition triggered by the sudden quench of a spatially disordered potential in a 2D interacting Bose gas using a relatively simple approach based on a random Gross-Pitaevskii equation. This allows us to explore two yet poorly understood problems: (1) How 2D systems dynamically evolve toward the vicinity of a KT transition depending on the quench parameters, and (2) once equilibrium is established, how is the transition affected by the disorder? To address the first question, we numerically study the full time evolution of the coherence function and the thermalization time of the Bose gas. This allows us to explain, in particular, findings of the recent experiment [11]. In the second problem, we characterize the long-time equilibrium transition line as a function of the disorder and compare it with state-of-the-art theoretical predictions. We finally investigate two core properties of the KT transition, the finite value of the superfluid density and the divergence of the correlation length and find evidence for their universality in the presence of disorder.

Consider a dilute 2D Bose gas initially prepared in a plane-wave state $|\boldsymbol{k}_0\rangle$, i.e., an eigenstate of the free Hamiltonian. From now on we choose the initial momentum $\boldsymbol{k}_0$ oriented along x. At time $t = 0$, we assume that the gas is suddenly subjected to a 2D disorder potential $V(\boldsymbol{r} = x, y)$, which we model by an uncorrelated random Gaussian function with zero mean: $\overline{V(\boldsymbol{r})} = 0$ and $\overline{V(\boldsymbol{r})V(\boldsymbol{r}')} = \gamma\delta(\boldsymbol{r} - \boldsymbol{r}')$ where the overbar refers to the disorder average and γ is the disorder strength. The latter defines an energy scale γm, where m is the mass of the particles and we have set $\hbar = 1$. From $t = 0$ onward, $|\boldsymbol{k}_0\rangle$ is no longer an eigenstate of the problem so that the Bose gas starts evolving in time. We describe this evolution using the nonlinear Schrödinger equation,

$$i\,\partial_t\psi = -\nabla^2\psi/(2m) + V\psi + gN|\psi|^2\psi, \tag{1}$$

where $\psi = \psi(\boldsymbol{r}, t)$ is the wave function. The latter is normalized according to $\int d^2\boldsymbol{r}|\psi(\boldsymbol{r}, t)|^2 = 1$, and the prequench state is $\psi(\boldsymbol{r}, 0) = 1/\sqrt{\Omega}\exp(i\boldsymbol{k}_0\cdot\boldsymbol{r})$ with Ω as the volume of the system. The particle density is $\rho_0 = N/\Omega$. In practice, this quench protocol can be realized by cooling a Bose gas to low temperatures, transferring it a momentum, and subjecting it to an optical random potential [58]. The problem is also relevant in the context of nonlinear paraxial optics where $\boldsymbol{k}_0$ refers to the transverse wave vector of a laser impinging on a nonlinear medium at finite angle of incidence [40,41,59]. In that case, the disorder can be realized by imprinting 2D refractive-index fluctuations on the (x, y) plane [60,61].

Averaging the solutions of the random Eq. (1) over many realizations of $V(\boldsymbol{r})$ allows us to effectively go beyond the mean-field level and capture the complex dynamics of the Bose gas, including the KT transition. In spirit, this approach is similar to a truncated Wigner approximation where one samples a random initial state [62]. To describe the gas dynamics, we study the average coherence function,

$$g_1(\boldsymbol{r}, t) = \overline{\psi^*(0, t)\psi(\boldsymbol{r}, t)}/\overline{|\psi(\boldsymbol{r}, t)|^2}. \tag{2}$$

To evaluate g_1, we numerical propagate the wave function with Eq. (1) using a split-step algorithm from which we compute the momentum distribution [29]. g_1 follows from inverse Fourier transformation and disorder averaging. In our simulations, we discretize space on a rectangular lattice $\Omega = L \times L$ with step $\delta = 1.5$ and use periodic boundary conditions. Throughout the Letter, lengths, momenta, and energies are given in units of a, a^{-1}, and $1/(ma^2)$, where a is an arbitrary unit length. The behavior of g_1 as a function of time is entirely governed by three independent energy scales characterizing the postquench state: the kinetic, disorder, and interaction energies $k_0^2/2m$, γm, and $g\rho_0$, respectively [63]. We first show in Fig. 1 g_1 vs time for two different sets $(k_0^2/2m, \gamma m, g\rho_0)$. In panel (a), $\gamma m \ll g\rho_0$. In this low-energy regime (weak disorder quench), g_1 quickly exhibits an algebraic scaling,

$$g_1(\boldsymbol{r}, t) \sim (\xi/r)^{\alpha(t)}. \tag{3}$$

The algebraic exponent $\alpha(t)$ is shown in the inset of Fig. 1(a). It decreases in time and saturates when $t \sim 10^4\tau_g$ with $\tau_g = 1/(g\rho_0)$, indicating that the system has reached its final equilibrium state where the gas behaves as a *superfluid*. The time evolution of $\alpha(t)$ features a slow crossover from a prethermal regime at a short time, where $\alpha(t) \simeq \gamma m/4\pi g\rho_0$ [30], to a finite-temperature superfluid state at a long time, where $\alpha(t) \to \alpha(\infty)$ is related to the superfluid density as will be investigated below. At a short time, the algebraic decay is limited by the Lieb-Robinson bound $r = 2c_s t$, where $c_s = \sqrt{g\rho_0/m}$ is the speed of sound, whereas at a long time it is limited by the system size.

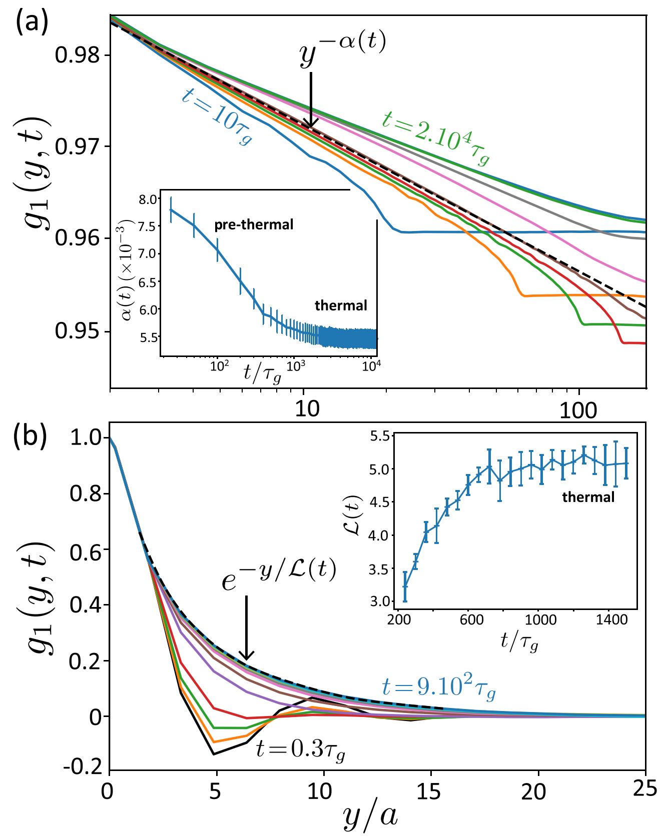

FIG. 1. Coherence function $g_1(x = 0, y, t)$ vs time of a 2D Bose gas after a disorder quench for two sets of initial conditions (the first and last time steps are indicated in each plot) (a) $\gamma m = 0.09$, $g\rho_0 = 1$, and $k_0 = 0$ ($\gamma m/g\rho_0 \ll 1$): shortly after the quench, g_1 decays algebraically, Eq. (3). At a short time, the gas lies in a prethermal regime: the algebraic exponent $\alpha(t) \simeq \gamma m/4\pi g\rho_0$ (dashed line), then decreases slowly, and g_1 is limited by a Lieb-Robinson bound. At a long time, thermal equilibrium establishes: $\alpha(t) \to \alpha(\infty)$ and g_1 is only limited by the system size. The inset shows the full evolution of $\alpha(t)$. (b) $\gamma m = 0.09$, $g\rho_0 = 0.003$, and $k_0 = 0.754$ ($\gamma m/g\rho_0 \gg 1$): shortly after the quench, g_1 acquires an exponential shape, Eq. (4), with a correlation length $\mathcal{L}(t)$ slowly increasing with time. All data are averaged over 128 disorder realizations and over system sizes $L \in [75, 100]$ (a) and $L \in [350, 400]$ (b). Space and time units are explained in the main text.

Figure 1(b) shows $g_1(\boldsymbol{r}, t)$ for a different initial condition such that $\gamma m \gg g\rho_0$. In this regime, the coherence function right after the quench is governed by disorder scattering and is nonuniversal [31]. Very quickly though, particle interactions take over and induce an exponential coherence that persists over all times,

$$g_1(\boldsymbol{r}, t) \sim \exp[-r/\mathcal{L}(t)]. \tag{4}$$

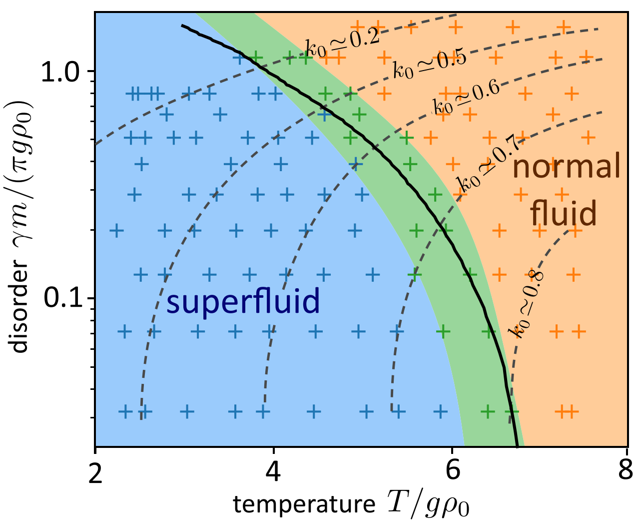

FIG. 2. Equilibrium phase diagram reached by the 2D Bose gas a long time after the disorder quench, deduced from the spatial decay of $g_1(\boldsymbol{r}, t \to \infty)$. Each cross symbol corresponds to a given set $(k_0^2/2m, \gamma m, g\rho_0)$ with γm ranging from 0.01 to 0.49 and k_0 from 0 to 0.9. Here $g\rho_0 = 0.1$ is fixed, and we use a system size $L = 400$ and 64 disorder realizations for averaging. The dashed curves indicate the points of constant k_0 values, and the solid curve is the theoretical prediction for the Kosterlitz-Thouless transition line $(\gamma m, T_{\rm KT})$, Eq. (5).

The correlation length $\mathcal{L}(t)$ is shown in the inset of Fig. 1(b). It increases in time and saturates when $t \sim 10^3\tau_g$, the Bose gas now reaching a purely *thermal* state. Whereas full thermalization takes some time to establish, it is remarkable that, in this regime of stronger disorder, the exponential coherence emerges shortly after the quench. This result explains the recent observations of Ref. [11] where a transition from algebraic to exponential coherence was observed in a nonequilibrium fluid of light despite the system being probed at relatively short times.

This dynamical analysis shows that after the quench the Bose gas thermalizes into a phase that crucially depends on the initial conditions $(k_0^2/2m, \gamma m, g\rho_0)$. To characterize the final equilibrium state more exhaustively, we have performed a systematic analysis of the coherence function vs time for a large set of initial conditions. For each of those, we have determined whether $g_1(\boldsymbol{r}, t \to \infty)$ behaves exponentially or algebraically [64]. The result of this analysis is summarized by the phase diagram in Fig. 2. The various equilibrium phases are represented as a function of the disorder energy γm and the temperature T at fixed $g\rho_0$. Here T is the effective temperature acquired by the Bose gas after its self-equilibration and is determined by the initial conditions. To find it, we have computed numerically the occupation number at energy ϵ, $N_\epsilon(t) = \rho_0\overline{\langle\psi(t)|\delta(\epsilon - H_0)|\psi(t)\rangle}/\nu_\epsilon$, where $H_0 = -\nabla^2/(2m) + V$ and ν_ϵ is the average density of state per unit volume. Whatever phase it lies in at a long time, the Bose gas always contains a certain fraction of thermal particles. These particles occupy the states of highest energy, corresponding to $N_{\epsilon\to\infty}(\infty) \sim T/(\epsilon - \mu)$, where μ is the chemical potential. This asymptotic law is the so-called Rayleigh-Jeans distribution, which describes the thermal equilibrium of classical-field theories [32,34,35]. Therefore, by examining $N_\epsilon(\infty)$ at large ϵ, one can infer both T and μ for a given $(k_0^2/2m, \gamma m, g\rho_0)$ [64]. In practice, at fixed γm and $g\rho_0$, higher temperatures are achieved by increasing k_0 as illustrated by the equi-k_0 lines in Fig. 2.

Figure 2 shows that the long-time equilibrium state crosses from a superfluid to a normal fluid as T is increased. A similar transition is also observed if the ratio $\gamma m/g\rho_0$ is increased at fixed temperature. The set of parameters for which both an algebraic or an exponential decay can equally well describe g_1 due to numerical uncertainties defines the central green region in the phase diagram [64]. It is in this region that we expect a Kosterlitz-Thouless transition to occur. To confirm it, we have evaluated semianalytically γ vs the critical temperature $T_{\rm KT}$ of the KT transition, in the spirit of the recent work [23]. The approach consists of calculating the superfluid density $\rho_s(T)$ on the superfluid side of the transition in the presence of disorder using Bogoliubov theory [65,66] and extrapolating the result to the transition point assuming the Nelson-Kosterlitz relation $\rho_s(T_{\rm KT}) = 2mT_{\rm KT}/\pi$. This relation, well known in the homogeneous case, describes a universal jump of the superfluid density at the transition [67]. Below we will verify its validity numerically in the presence of disorder. At weak disorder $\gamma m \ll g\rho_0$, this calculation provides

$$\gamma m = \frac{4\pi g\rho_0}{I_1}\left[1 - \frac{T_{\rm KT}}{T_d}(4 + I_2)\right], \tag{5}$$

where $T_d = 2\pi\rho_0/m$, $I_1 = \int d\epsilon\, 4g\rho_0(\nu_\epsilon/\nu)/(\epsilon + 3g\rho_0 - \mu)^2$ and $I_2 = \int d\epsilon(\nu_\epsilon/\nu)/(\epsilon + 3g\rho_0 - \mu)$ with $\nu = m/2\pi$ [64]. In these integrals, ϵ is bounded from above by the lattice energy $4/(m\delta^2)$. We also restrict ourselves to $\epsilon > 0$, the density of states being very small at negative energy. In the homogeneous limit $(\gamma, \delta \to 0)$, Eq. (5) reduces to $T_{\rm KT} = T_d/\ln(e^4 T_d/g\rho_0)$, very close to the value of $\simeq T_d/\ln(60T_d/g\rho_0)$ obtained in Monte Carlo simulations [57,68]. Because Eq. (5) holds at weak disorder only, however, it is insufficient to accurately capture our simulations. To solve this issue, we have further included the next-order disorder correction to Eq. (5) [69,70] and have also accounted for the disorder dependence of ν_ϵ [64]. With these corrections, Eq. (5) becomes an implicit equation for γ which needs to be numerically solved. This yields the critical curve shown in Fig. 2 where we have adjusted $g\rho_0 \simeq 0.122$. This analysis confirms the validity of Eq. (5) within 20% accuracy, a value that might be improved by working at weaker interaction.

To further characterize the KT transition emerging after the quench, we have studied two critical observables. The first one is the superfluid fraction $\rho_s(T = T_{\rm KT}) = 2mT_{\rm KT}/\pi$ at the transition, which in the absence of disorder is known to undergo a jump associated with a proliferation of vortices. This is also the relation we have assumed above for deriving the critical line, Eq. (5). To test it, we have numerically computed the algebraic exponent $\alpha(t \to \infty)$ of $g_1(\boldsymbol{r}, t \to \infty)$, see Eq. (3), for various disorder strengths and temperatures in the vicinity of $T_{\rm KT}$. In homogeneous systems, $\alpha(\infty) = 1/\rho_s(T)\lambda_T^2$ with $\lambda_T = \sqrt{2\pi/mT}$ as the thermal wavelength. The jump of ρ_s at the transition then corresponds to $\alpha(\infty) = 1/4$. The results of this analysis are shown in Fig. 3(a). As $T \to T_{\rm KT}$, we indeed observe that points at different γ tend to all satisfy $\alpha(\infty) = 1/4$. A second central property of the KT transition

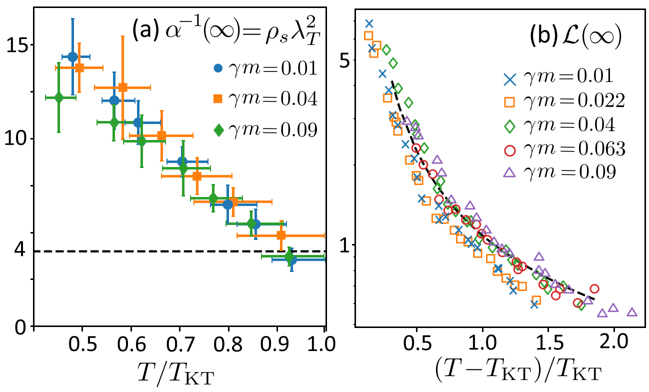

FIG. 3. (a) Inverse of the algebraic exponent $\alpha(\infty)$ on the superfluid side of the KT transition, extracted from $g_1(\boldsymbol{r}, t \to \infty)$ for different temperatures and disorder strengths. The plot suggests $\alpha \simeq 1/4$ near the transition, irrespective of γ. The dashed line pinpoints $\alpha^{-1}(\infty) = 4$. (b) Correlation length $\mathcal{L}(\infty)$ extracted from $g_1(\boldsymbol{r}, t \to \infty)$ on the normal side, for different temperatures and disorder strengths. In both plots parameters are the same as in Fig. 2, namely $g\rho_0 = 0.1$, $L = 400$, and we average over 64 disorder realizations. The critical temperature T_{KT} is found numerically by taking the average of the two extreme points lying in the critical area in Fig. 2. The dashed curve is a fit to Eq. (6).

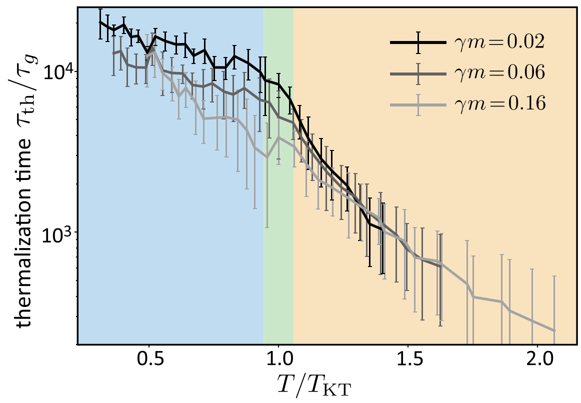

FIG. 4. Thermalization time vs temperature for three disorder strengths. Parameters are the same as in Fig. 2 except the system size $L = 300$.

is the fast divergence of the correlation length $\mathcal{L}$, see Eq. (4), in the vicinity of the transition [71],

$$\mathcal{L}(\infty) \sim \sqrt{\frac{T_{\mathrm{KT}}}{T}} \exp\left[\sqrt{\frac{\zeta T_{\mathrm{KT}}}{T - T_{\mathrm{KT}}}}\right]. \tag{6}$$

To test Eq. (6) in the presence of disorder, we have extracted $\mathcal{L}(\infty)$ from $g_1(\boldsymbol{r}, t \to \infty)$ for various disorder strengths and temperature close to T_{KT}. The results, shown in Fig. 3(b), remarkably fall on the same universal curve. A fit (dashed curve) further demonstrates a good agreement with Eq. (6). Overall, these results point toward a universal character of the KT transition in the presence of disorder, once the critical temperature has been properly rescaled according to Eq. (5).

We have, finally, analyzed the thermalization time τ_{th} needed for the system to equilibrate after the quench. To estimate it, we use the empirical numerical criterion that beyond τ_{th}, the area $A(t) = \int_0^{L/2} dy\, g_1(x = 0, y, t)$ does not vary significantly in time whatever the quench parameters, i.e., for any point of the phase diagram in Fig. 2. In practice, we fit $A(t)$ with a function of the form $B - C/(t + D)^2$ and define τ_{th} as the time for which this function reaches 95% of its maximum B. The uncertainty on the fit parameters provide error bars for the determination of τ_{th}. Figure 4 shows τ_{th} vs temperature for different γm's. Whereas $\tau_{\mathrm{th}}(T)$ decreases nearly exponentially on the normal side, we observe a sizable increase in the thermalization time as one crosses from the normal to the superfluid phase. Note also that except perhaps at strong disorder, in the superfluid region disorder tends to "help" the system to thermalize faster, a phenomenon that has been previously pointed out for interacting bosons in dimension one [73]. This nontrivial outcome is the result of a compromise between two antagonistic effects, the disorder that makes the system more ergodic after the quench, and the interactions that drive a superfluid state less sensitive to the disorder.

In conclusion, we have characterized the dynamical equilibration of 2D interacting Bose gases subjected a disorder potential quench, exploring both the nonequilibrium and the equilibrium facets of the problem and providing a benchmark for future experiments on atomic or photonic disordered fluids. An analysis of the dynamical exponents governing the approach to equilibrium would be an interesting challenge for future work as well as the possible existence of a finite-temperature localized or insulating phase at stronger disorder, pointed out in Ref. [23]. Whereas it remains unclear whether signatures of such a phase could be found from a classical-field description, use of a nonequilibrium approach to describe it is best suited, given the fundamental dynamical nature of the many-body localization.

N.C. acknowledges the Agence Nationale de la Recherche (Grant No. ANR-19-CE30-0028-01 CONFOCAL) for financial support and discussions with A. de Luca and F. Alet.

[1] A. Polkovnikov, K. Sengupta, A. Silva, and M. Vengalattore, Colloquium: Nonequilibrium dynamics of closed interacting quantum systems, Rev. Mod. Phys. **83**, 863 (2011).
[2] C. Gogolin and J. Eisert, Equilibration, thermalisation, and the emergence of statistical mechanics in closed quantum systems, Rep. Prog. Phys. **79**, 056001 (2016).
[3] L. D'Alessio, Y. Kafri, A. Polkovnikov, and M. Rigol, From quantum chaos and eigenstate thermalization to statistical mechanics and thermodynamics, Adv. Phys. **65**, 239 (2016).
[4] J. M. Deutsch, Eigenstate thermalization hypothesis, Rep. Prog. Phys. **81**, 082001 (2018).
[5] M. Ueda, Quantum equilibration, thermalization and prethermalization in ultracold atoms, Nat. Rev. Phys. **2**, 669 (2020).

[6] J. Berges, A. Rothkopf, and J. Schmidt, Nonthermal Fixed Points: Effective Weak Coupling for Strongly Correlated Systems Far from Equilibrium, Phys. Rev. Lett. **101**, 041603 (2008).

[7] A. Piñeiro Orioli, K. Boguslavski, and J. Berges, Universal self-similar dynamics of relativistic and nonrelativistic field theories near nonthermal fixed points, Phys. Rev. D **92**, 025041 (2015).

[8] A. N. Mikheev, C.-M. Schmied, and T. Gasenzer, Low- energy effective theory of nonthermal fixed points in a multicomponent Bose gas, Phys. Rev. A **99**, 063622 (2019).

[9] J. Berges, S. Borsányi, and C. Wetterich, Prethermalization, Phys. Rev. Lett. **93**, 142002 (2004).

[10] S. Trotzky, Y.-A. Chen, A. Flesch, I. P. McCulloch, U. Schollwöck, J. Eisert, and I. Bloch, Probing the relaxation towards equilibrium in an isolated strongly correlated one-dimensional Bose gas, Nat. Phys. **8**, 325 (2012).

[11] M. Abuzarli, N. Cherroret, T. Bienaimé, and Q. Glorieux, Non-equilibrium pre-thermal states in a two-dimensional photon fluid, arXiv:2203.07399.

[12] M. Gring, M. Kuhnert, T. Langen, T. Kitagawa, B. Rauer, M. Schreitl, I. Mazets, D. A. Smith, E. Demler, and J. Schmiedmayer, Relaxation and prethermalization in an isolated quantum system, Science **337**, 1318 (2012).

[13] M. Kollar, F. A. Wolf, and M. Eckstein, Generalized Gibbs ensemble prediction of prethermalization plateaus and their relation to nonthermal steady states in integrable systems, Phys. Rev. B **84**, 054304 (2011).

[14] T. Langen, S. Erne, R. Geiger, B. Rauer, T. Schweigler, M. Kuhnert, W. Rohringer, I. E. Mazets, T. Gasenzer, and J. Schmiedmayer, Experimental observation of a generalized Gibbs ensemble, Science **348**, 207 (2015).

[15] M. Van Regemortel, H. Kurkjian, M. Wouters, and I. Carusotto, Prethermalization to thermalization crossover in a dilute Bose gas following an interaction ramp, Phys. Rev. A **98**, 053612 (2018).

[16] K. Mallayya and M. Rigol, Quantum Quenches and Relaxation Dynamics in the Thermodynamic Limit, Phys. Rev. Lett. **120**, 070603 (2018).

[17] K. Mallayya, M. Rigol, and W. De Roeck, Prethermalization and Thermalization in Isolated Quantum Systems, Phys. Rev. X **9**, 021027 (2019).

[18] M. Buchhold, M. Heyl, and S. Diehl, Prethermalization and thermalization of a quenched interacting Luttinger liquid, Phys. Rev. A **94**, 013601 (2016).

[19] D. A. Abanin, E. Altman, I. Bloch, and M. Serbyn, Colloquium: Many-body localization, thermalization, and entanglement, Rev. Mod. Phys. **91**, 021001 (2019).

[20] I. V. Gornyi, A. D. Mirlin, and D. G. Polyakov, Interacting Electrons in Disordered Wires: anderson Localization and Low-T Transport, Phys. Rev. Lett. **95**, 206603 (2005).

[21] D. M. Basko, I. L. Aleiner, and B. L. Altshuler, Metal-insulator transition in a weakly interacting many-electron system with localized single-particle states, Ann. Phys. (NY) **321**, 1126 (2006).

[22] J.-y. Choi, J.-Y. Choi, S. Hild, J. Zeiher, P. Schauß, A. Rubio-Abadal, T. Yefsah, V. Khemani, D. A. Huse, I. Bloch, and C. Gross, Exploring the many-body localization transition in two dimensions, Science **352**, 1547 (2016).

[23] G. Bertoli, V. P. Michal, B. L. Altshuler, and G. V. Shlyapnikov, Finite-Temperature Disordered Bosons in Two Dimensions, Phys. Rev. Lett. **121**, 030403 (2018).

[24] H. Théveniaut, Z. Lan, G. Meyer, and F. Alet, Transition to a many-body localized regime in a two-dimensional disordered quantum dimer model, Phys. Rev. Research **2**, 033154 (2020).

[25] F. Pietracaprina and Fabien Alet, Probing many-body localization in a disordered quantum dimer model on the honeycomb lattice, Sci. Post Phys. **10**, 044 (2021).

[26] G. Kopidakis, S. Komineas, S. Flach, and S. Aubry, Absence of Wave Packet Diffusion in Disordered Nonlinear Systems, Phys. Rev. Lett. **100**, 084103 (2008).

[27] A. S. Pikovsky and D. L. Shepelyansky, Destruction of Anderson Localization by a Weak Nonlinearity, Phys. Rev. Lett. **100**, 094101 (2008).

[28] N. Cherroret, B. Vermersch, J. C. Garreau, and D. Delande, How Nonlinear Interactions Challenge the Three-Dimensional Anderson Transition, Phys. Rev. Lett. **112**, 170603 (2014).

[29] T. Scoquart, T. Wellens, D. Delande, and N. Cherroret, Quench dynamics of a weakly interacting disordered Bose gas in momentum space, Phys. Rev. Research **2**, 033349 (2020).

[30] T. Scoquart, P.-É. Larré, D. Delande, and N. Cherroret, Weakly interacting disordered Bose gases out of equilibrium: From multiple scattering to superfluidity, Europhys. Lett. **132**, 66001 (2020).

[31] N. Cherroret, T. Scoquart, and D. Delande, Coherent multiple scattering of out-of-equilibrium interacting Bose gases, Ann. Phys. **435**, 168543 (2021).

[32] C. Connaughton, C. Josserand, A. Picozzi, Y. Pomeau, and S. Rica, Condensation of Classical Nonlinear Waves, Phys. Rev. Lett. **95**, 263901 (2005).

[33] J. Berges and D. Sexty, Bose-Einstein Condensation in Relativistic Field Theories Far from Equilibrium, Phys. Rev. Lett. **108**, 161601 (2012).

[34] N. Cherroret, T. Karpiuk, B. Grémaud, and C. Miniatura, Thermalization of matter waves in speckle potentials, Phys. Rev. A **92**, 063614 (2015).

[35] P. Aschieri, J. Garnier, C. Michel, V. Doya, and A. Picozzi, Condensation and thermalization of classical optical waves in a waveguide, Phys. Rev. A **83**, 033838 (2011).

[36] A. Chiocchetta, P. É. Larré, and I. Carusotto, Thermalization and Bose-Einstein condensation of quantum light in bulk nonlinear media, Europhys. Lett. **115**, 24002 (2016).

[37] V. Shukla and S. Nazarenko, Non-equilibrium Bose-Einstein Condensation, Phys. Rev. A **105**, 033305 (2022).

[38] P. Haldar, S. Mu, B. Georgeot, J. Gong, C. Miniatura, and G. Lemarié, Prethermalization and wave condensation in a nonlinear disordered Floquet system, arXiv:2109.14347.

[39] S. Nazarenko, *Wave Turbulence*, Lecture Notes in Physics, Vol. 825 (Springer, Heidelberg, Berlin, 2011).

[40] N. Šantić, A. Fusaro, S. Salem, J. Garnier, A. Picozzi, and R. Kaiser, Nonequilibrium Precondensation of Classical Waves in Two Dimensions Propagating through Atomic Vapors, Phys. Rev. Lett. **120**, 055301 (2018).

[41] C. Sun, S. Jia, C. Barsi, S. Rica, A. Picozzi, and J. W Fleischer, Observation of the kinetic condensation of classical waves, Nat. Phys. **8**, 470 (2012).

[42] L. G. Wright, Z. Liu, D. A. Nolan, M.-J. Li, D. N. Christodoulides, and F. W. Wise, Self-organized instability in graded-index multimode fibres, Nat. Photonics **10**, 771 (2016).

[43] K. Krupa, A. Tonello, B. M. Shalaby, M. Fabert, A. Barthélémy, G. Millot, S. Wabnitz, and V. Couderc, Spatial beam self-cleaning in multimode fibres, Nat. Photonics **11**, 237 (2017).
[44] K. Baudin, A. Fusaro, K. Krupa, J. Garnier, S. Rica, G. Millot, and A. Picozzi, Classical Rayleigh-Jeans Condensation of Light Waves: Observation and Thermodynamic Characterization, Phys. Rev. Lett. **125**, 244101 (2020).
[45] J. M. Kosterlitz and D. J. Thouless, Ordering, metastability and phase transitions in two-dimensional systems, J. Phys. C **6**, 1181 (1973).
[46] D. J. Bishop and J. D. Reppy, Study of the Superfluid Transition in Two-Dimensional $_4$He Films, Phys. Rev. Lett. **40**, 1727 (1978).
[47] Z. Hadzibabic, P. Krüger, M. Cheneau, B. Battelier, and J. Dalibard, Berezinskii-Kosterlitz-Thouless crossover in a trapped atomic gas, Nature (London) **441**, 1118 (2006).
[48] P. Cladé, C. Ryu, A. Ramanathan, K. Helmerson, and W. D. Phillips, Observation of a 2D Bose Gas: From Thermal to Quasicondensate to Superfluid, Phys. Rev. Lett. **102**, 170401 (2009).
[49] S. Tung, G. Lamporesi, D. Lobser, L. Xia, and E. A. Cornell, Observation of the Presuperfluid Regime in a Two-Dimensional Bose Gas, Phys. Rev. Lett. **105**, 230408 (2010).
[50] T. Yefsah, R. Desbuquois, L. Chomaz, K. J. Günter, and J. Dalibard, Exploring the Thermodynamics of a Two-Dimensional Bose Gas, Phys. Rev. Lett. **107**, 130401 (2011).
[51] P. Christodoulou, M. Gałka, N. Dogra, R. Lopes, J. Schmitt, and Z. Hadzibabic Observation of first and second sound in a BKT superfluid, Nature (London) **594**, 191 (2021).
[52] S. Nazarenko, M. Onorato, and D. Proment, Bose-Einstein condensation and Berezinskii-Kosterlitz-Thouless transition in the two-dimensional nonlinear Schrödinger model, Phys. Rev. A **90**, 013624 (2014)
[53] G. Situ and J. W. Fleischer, Dynamics of the Berezinskii-Kosterlitz-Thouless transition in a photon fluid, Nat. Photonics **14**, 517 (2020).
[54] T. Plisson, B. Allard, M. Holzmann, G. Salomon, A. Aspect, P. Bouyer, and T. Bourdel, Coherence properties of a two-dimensional trapped Bose gas around the superfluid transition, Phys. Rev. A **84**, 061606(R) (2011).
[55] B. Allard, T. Plisson, M. Holzmann, G. Salomon, A. Aspect, P. Bouyer, and T. Bourdel, Effect of disorder close to the superfluid transition in a two-dimensional Bose gas, Phys. Rev. A **85**, 033602 (2012).
[56] T. Bourdel, Phase diagrams of 2D and 3D disordered Bose gases in the local density approximation, Phys. Rev. A **86**, 063626 (2012).
[57] G. Carleo, G. Boéris, M. Holzmann, and L. Sanchez-Palencia, Universal Superfluid Transition and Transport Properties of Two-Dimensional Dirty Bosons, Phys. Rev. Lett. **111**, 050406 (2013).
[58] F. Jendrzejewski, K. Müller, J. Richard, A. Date, T. Plisson, P. Bouyer, A. Aspect, and V. Josse, Coherent Backscattering of Ultracold Atoms, Phys. Rev. Lett. **109**, 195302 (2012).
[59] Q. Fontaine, T. Bienaimé, S. Pigeon, E. Giacobino, A. Bramati, and Q. Glorieux, Observation of the Bogoliubov Dispersion in a Fluid of Light, Phys. Rev. Lett. **121**, 183604 (2018).
[60] T. Schwartz, G. Bartal, S. Fishman, and M. Segev, Transport and Anderson localization in disordered two-dimensional photonic lattices, Nature (London) **446**, 52 (2007).
[61] N. Cherroret, Coherent multiple scattering of light in (2+1) dimensions, Phys. Rev. A **98**, 013805 (2018).
[62] A. Sinatra, C. Lobo, and Y. Castin, The truncated Wigner method for Bose-condensed gases: Limits of validity and applications, J. Phys. B: At., Mol. Opt. Phys. **35**, 3599 (2002).
[63] The lattice energy $1/(m\delta^2)$ amounts to a global scaling factor and is, thus, fixed throughout the Letter.
[64] See Supplemental Material at http://link.aps.org/supplemental/10.1103/PhysRevA.106.L021301, which includes Ref. [72] for details on the computation of the equilibrium temperature and chemical potential, the construction of the phase diagram, and the derivation of Eq. (5).
[65] H.-F. Meng, Quantum theory of the two-dimensional interacting-boson system, Phys. Rev. B **49**, 1205 (1994).
[66] J. Keeling, Response functions and superfluid density in a weakly interacting Bose gas with nonquadratic dispersion, Phys. Rev. B **74**, 155325 (2006).
[67] D. R. Nelson and J. M. Kosterlitz, Universal Jump in the Superfluid Density of Two-Dimensional Superfluids, Phys. Rev. Lett. **39**, 1201 (1977).
[68] N. Prokof'ev, O. Ruebenacker, and B. Svistunov, Critical Point of a Weakly Interacting Two-Dimensional Bose Gas, Phys. Rev. Lett. **87**, 270402 (2001).
[69] V. I. Yukalov and R. Graham, Bose-Einstein-condensed systems in random potentials, Phys. Rev. A **75**, 023619 (2007).
[70] V. I. Yukalov, E. P. Yukalova, K. V. Krutitsky, and R. Graham, Bose-Einstein condensed gases in arbitrarily strong random potentials, Phys. Rev. A **76**, 053623 (2007).
[71] Z. Hadzibabic and J. Dalibard, Two-dimensional Bose fluids: An atomic physics perspective, Riv. Nuovo Cim. **34**, 389 (2011).
[72] M. I. Trappe, D. Delande, and C. A. Mueller, Semiclassical spectral function for matter waves in random potentials, J. Phys. A: Math. Theor. **48**, 245102 (2015).
[73] M. Tavora, A. Rosch, and A. Mitra, Quench Dynamics of One-Dimensional Interacting Bosons in a Disordered Potential: Elastic Dephasing and Critical Speeding-Up of Thermalization, Phys. Rev. Lett. **113**, 010601 (2014).